

Hybrid Shubnikov–de Haas-photoluminescence analysis of two-dimensional electron density in strained quantum well structures with heavily doped contact layers

Michael L. Lovejoy and Jerry A. Simmons
Sandia National Laboratories, Albuquerque, New Mexico 87185

Pin Ho and Paul A. Martin
Martin Marietta Electronics Laboratory, Syracuse, New York 13221

(Received 14 January 1994, accepted for publication 13 April 1994)

A hybrid analysis technique is presented to accurately extract the two-dimensional (2D) electron density of PHEMT structures in which multiple subbands are occupied and severe parallel conduction by heavily doped contact layers occurs. Complications due to shorted Hall voltages by the parallel contact layer, which precludes simple Hall analysis, and to multiple subband occupation, which requires high magnetic-field sweeps in Shubnikov–de Haas (SdH) measurements, are eliminated by this hybrid analysis that combines SdH measurements with photoluminescence measurements to extract the total 2D density. Comparisons with other methods demonstrate the high accuracy of this new technique.

The 2D electron density in the quantum well of strained quantum well field effect transistors (SQWFETs), or equivalently pseudomorphic high electron mobility transistors (PHEMTs), is an important parameter for device performance. Figures of merit such as the drain-source current and transconductance are proportional to the carrier concentration (n_{2D}) in the well, hence accurate n_{2D} data are needed for structure optimization and reliable device modeling. Measurement of n_{2D} is complicated by two factors. First, high-performance PHEMTs require heavily doped cap layers to realize low-resistance ohmic contacts.^{1,2} This layer presents a conduction path parallel to the two-dimensional (2D) gas conduction channel in the SQW. In general, Hall effect and Shubnikov–de Haas (SdH) responses of the two layers are different; consequently, the measured Hall and longitudinal voltages are nonlinear, intermediate values which do not accurately characterize either layer. Second, high performance also requires high carrier concentrations which result in multiple subbands being occupied.² SdH oscillations from individual subbands are superimposed, which makes measurement and data analysis difficult. Techniques to deduce the 2D gas density from these convolved signals have been developed,^{2,3} but there is a need for a simple, accurate technique to extract the concentration. In this paper we combine SdH measurements with steady-state photoluminescence (PL) measurements in a hybrid analysis technique (SdH-PL) to extract the 2D gas density of PHEMT structures with severe parallel conduction and multiple subband occupation.

This new technique has advantages over commonly employed techniques. The iterative-etch/Hall-effect measurement technique, where the cap layer is sequentially etched to eliminate the parallel conduction path and Hall measurements are taken at each etch step, has the problem that as the cap is removed, the carrier concentration varies due to changes in band bending. Consequently, it is difficult to identify the correct etch depth and corresponding carrier concentration that characterizes the device. Another technique is the variable magnetic-field (B) Hall-effect measurement in

which the Hall voltage is fit with a four parameter model;⁴ accuracy can be reduced with fits in such a large parameter space. A third technique is SdH analysis which requires identifying multiple frequencies of oscillations in high-performance PHEMTs where multiple quantum well subbands are occupied. In principle, the frequencies can be resolved by taking the Fourier power spectrum³ or twice differentiating² the magnetoresistance. The Fourier power spectrum technique can require large B sweeps as high as 20 T and the second derivative analysis requires very low levels of noise to resolve both frequencies. A recently reported technique fits to PL spectra;¹ however, this technique requires identifying subtle features in PL-line shape. In contrast to these techniques, the hybrid SdH-PL technique employs measurements of the actual PHEMT structure, relatively low B strengths, excellent noise tolerance, and simple linear fits.

The hybrid SdH-PL analysis is based on the fact that local minima in the longitudinal magnetoresistivity occur when the Fermi energy is midway between Landau levels (LL)⁵ due to the suppression of scattering between the current carrying extended states of the LLs. For a system in an applied perpendicular B with two occupied subbands separated by energy E_{01} , which is diagrammed in Fig. 1, the minima occur with two periods of oscillations. The energy spacing of LLs is given by $\hbar\omega_c = \hbar eB/m^*$, where e is the

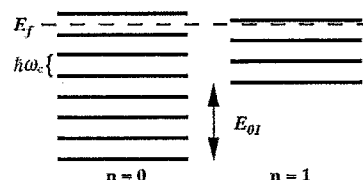


FIG. 1. Spin-degenerate Landau-level energy diagram showing the conditions for a local minimum in the longitudinal resistance with two subbands occupied.

electronic charge and m^* is the cyclotron resonance effective mass. As $\hbar\omega_c$ changes with B and because more LLs are occupied in the $n=0$ subband (see Fig. 1), the Fermi level passes through LLs more often for $n=0$; therefore, oscillations associated with the $n=0$ subband occur more rapidly than for the $n=1$ subband.

In general, the 2D carrier concentration is given by the integral over energy (E) of the density of states [$D(E)$] times the Fermi–Dirac distribution [$f(E)$]. For the 2D system depicted in Fig. 1 at low temperatures $kT \ll \hbar\omega_c$, one can approximate $f(E)$ by a step function and $D(E)$ for each subband as a summation of δ functions with LL degeneracies of $2eB/h$ where the factor of 2 is for spin degeneracy.² Thus $n_{2D} = (l_0 + l_1)2eB/h$ where, for the i th subband, l_i is the filling factor of spin-degenerate LLs and the carrier concentration is $l_i 2eB/h$. For the $n=0$ subband, l_0 is integer values at minima in the longitudinal resistance. In the SdH-PL technique l_0 is determined from the low-frequency oscillation in the longitudinal resistance and l_1 from $l_1 = l_0 - (E_{01}/\hbar\omega_c)$ which follows from Fig. 1 where $\hbar\omega_c$ is determined from cyclotron resonance measurements and E_{01} is extracted from low-temperature PL spectra which show two peaks when two subbands are occupied.¹ In actuality, disorder broadens the LLs and introduces localized states between them. However, since many LLs are occupied in PHEMT material at fields of several tesla, the above analysis is insensitive to the actual form of LL broadening. A sophisticated model (Ref. 5) such as one incorporating a Gaussian density of states could be used; however, we find the δ -functions density of states model to yield excellent results.

We demonstrate the accuracy of this technique by a comparison of carrier concentrations of several samples measured with multiple measurement techniques. The PHEMT material was grown in a Intevac GEN-II MBE system with nominally identical SQWs; however, one sample had a thin (30 Å) undoped contact layer and three other samples had thicker (350 Å) heavily doped ($N_D = 4 \times 10^{18} \text{ cm}^{-3}$) contact layers. It will be shown that the undoped GaAs cap facilitated contact formation but did not present a parallel conduction path while the heavily doped cap presented severe parallel conduction which distorts the SdH and Hall responses that characterize the 2D gas. The device structure is as follows: semi-insulating substrate, 1- μm undoped GaAs, 20 period 10-Å GaAs/200-Å $\text{Al}_{0.23}\text{Ga}_{0.77}\text{As}$ undoped superlattice, 50-Å $N_D = 9 \times 10^{17} \text{ cm}^{-3}$ $\text{Al}_{0.23}\text{Ga}_{0.77}\text{As}$, 50-Å undoped $\text{Al}_{0.23}\text{Ga}_{0.77}\text{As}$, 125-Å undoped $\text{In}_{0.22}\text{Ga}_{0.78}\text{As}$, 40-Å undoped $\text{Al}_{0.23}\text{Ga}_{0.77}\text{As}$, Si- δ -doped $4 \times 10^{12} \text{ cm}^{-2}$, 400-Å $N_D = 2 \times 10^{17} \text{ cm}^{-3}$ $\text{Al}_{0.23}\text{Ga}_{0.77}\text{As}$, and different GaAs contact layers. Devices for SdH measurements were Hall-bar structures fabricated by wet-etch mesa isolation and evaporated Au-Ge contacts annealed at 400 °C for 90 s. SdH measurements were made at 300 mK in a pumped ^3He cryostat, although measurements can be made as high as a liquid-helium temperatures. The B was sweep as high as 14 T; however, SDH-PL analyses utilized only 0–10 T data. PL measurements were performed at 2.2 K with 1.76 eV excitation and low power density. Iterative-etch/Hall measurements were performed with van der Pauw measurements at 77 K with at least six measurements. Since the carrier con-

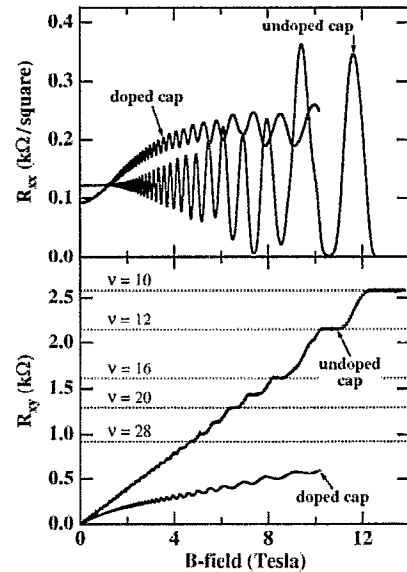


FIG. 2. Longitudinal resistance (R_{xx}) and transverse resistance (R_{xy}) for samples with nominally identical SQWs but different contact layers. The dependence on filling factor $\nu = 2(l_0 + l_1)$ where $R_{xy} = h/\nu e^2$ is also shown.

centration changes as the cap material is etched away, we report n_{2D} at the highest measured mobility value.

Transverse resistance (R_{xy}) and longitudinal resistance (R_{xx}) for samples with both an undoped cap and a doped cap are shown in Fig. 2. All doped cap samples exhibited similar characteristics. The effect of parallel conduction is clearly shown for these samples with nominally identical SQWs. While measured data for the sample with an undoped cap show the characteristic behavior of a 2D gas with plateaus in R_{xy} and with R_{xx} vanishing at high B , the doped cap devices do not exhibit either behavior. Parallel conduction smears out the plateaus in R_{xy} , significantly changes the low- B slope of R_{xy} , causes a “rollover” of both R_{xy} and R_{xx} as B increases, and also imposes a B -dependent R_{xx} background. R_{xx} clearly exhibits oscillations in $1/B$ corresponding to the $n=0$ subband and hints at a much slower, weaker oscillation due to the $n=1$ subband. Analysis of the undoped cap data is straightforward, however, analysis of the high-performance HEMT structure data is not—except with the SdH-PL analysis.

The undoped cap sample can be analyzed in a number of ways. First is a highly accurate technique to determine n_{2D} from the quantized Hall plateaus in R_{xy} , which is given by $h/\nu e^2$ where $\nu = 2(l_0 + l_1)$; the 2 is due to spin degeneracy.⁶ The effects of multiple subband occupation is evident in the R_{xy} characteristic where integer steps are skipped when the Fermi level passes through midpoints of LLs for both subbands simultaneously. Both of these phenomena are shown in Fig. 2 where the plateaus are indeed integer multiples of $h/2e^2$ except at ~ 6 and ~ 9 T where steps of $h/4e^2$ occur due to the combined responses of two occupied subbands. From each plateau value and the field at the corresponding minimum in $R_{xx}(B_{\min})$, n_{2D} is given by B_{\min}/eR_{xy} . For 20 plateaus in the range 2.2–10 T, n_{2D} is found to be $3.18 \pm 0.05 \times 10^{12} \text{ cm}^{-2}$; the uncertainty in this and subsequent calculations is the standard deviation from the mean

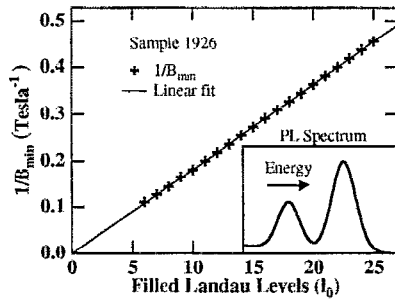


FIG. 3. Plot of inverse fields ($1/B_{\min}$) at which R_{xx} minima occur vs number of filled Landau levels (l_0). The integer l_0 is assigned by forcing the linear fit through the origin. The inset shows a representative PL spectrum (intensity vs energy) when two subbands are occupied.

value of a range of measurements on a given sample. Obviously from Fig. 2 this technique can not be applied when severe parallel conduction distorts the plateaus. The second technique, which is the conventional Hall-effect measurement and agrees with the earlier technique, calculates $n_{2D} = B/eR_{xy} = 3.18 \times 0.1 \times 10^{12} \text{ cm}^{-2}$ from the lower- B (0.25–2.75 T) R_{xy} data. We will show that parallel conduction due to doped caps can cause significant error in application of this technique. The third technique used for comparison is the iterative-etch/Hall-effect technique, which yielded $3.41 \times 10^{12} \text{ cm}^{-2}$. Deviations between the iterative-etch/Hall-effect measurement and nonetch techniques are expected since the band bending is changed as the device is etched. These data are compared to the results of SdH-PL analysis below.

Data for all four samples are analyzed with the SdH-PL technique as follows. The number of filled LLs in the $n=0$ subband (l_0) is determined from fits of $1/B_{\min}$ versus integer l_0 , as shown in Fig. 3 where the consecutive l_0 's assigned to each successive minima in R_{xx} is adjusted to force the linear fit to pass through the origin. The resulting fit determines l_0 at each B_{\min} . Shown in the inset of Fig. 3 is a representative PL spectrum that is used to extract the subband spacing (E_{01}) which is listed in Table I. The excellent consistency of E_{01} between samples indicates comparable indium composition in each SQW; in addition, TEM was employed to verify comparable SQW thicknesses. In general $l_1 = l_0 - (E_{01}/\hbar\omega_c)$ and $\hbar\omega_c$ can be determined from SdH-PL analysis of structures with undoped caps and quantized Hall analysis as discussed earlier. For comparison, we used the extrapolated CR mass ($0.056m_e$) that is reported for 0–0.2 mol fraction of indium⁷ and determined n_{2D} at each of the 20 B_{\min} values. The averages for the four samples studied are shown in Table

TABLE I. Subband energy separation (E_{01}) from PL and carrier concentrations from hybrid SdH-PL analyses and from iterative-etch Hall measurements.

| Sample | Cap doping | E_{01} (meV) | Hybrid SdH-PL (10^{12} cm^{-2}) | Iterative-etch Hall (10^{12} cm^{-2}) |
|--------|------------|----------------|---|---|
| 2063 | undoped | 76.1 | 3.23 ± 0.03 | 3.41 |
| 1912 | heavy | 77.0 | 3.43 ± 0.02 | 3.23 |
| 1920 | heavy | 77.2 | 3.38 ± 0.02 | 3.19 |
| 1926 | heavy | 78.3 | 3.49 ± 0.02 | 3.22 |

I with the standard deviation from the mean denoting the uncertainty.

SdH-PL analysis yielded excellent agreement with other independent analyses. For the undoped cap sample, agreement within a few percent and as good or better standard deviations were obtained with the SdH-PL technique when compared to techniques that are highly accurate when conduction occurs only in the 2D channel but are not applicable when parallel conduction occurs. As shown in Table I, the iterative-etch/Hall technique over estimates n_{2D} of the undoped sample by $\sim 6\%$. Also shown in Table I, the heavily doped cap results of SdH-PL analyses are in good agreement with iterative-etch/Hall measurements. In contrast to the undoped sample, the later technique under estimates n_{2D} . A possible cause of the different behavior may be differences in band bending that occurs as the cap is etch away; the depletion layer would extend much further into the structure when the cap is undoped as compared to being heavily doped. To show the error that results from a low- B data analysis, n_{2D} for the 1926-doped cap data was determined from the low- B slope. The result $n_{2D} = 5.13 \times 10^{12} \text{ cm}^{-2}$ is a factor of 1.5 greater than deduced by the hybrid SdH-PL analysis and iterative-etch techniques. This error is due to parallel conduction in the heavily doped cap layer of these devices.

In conclusion, we have presented a hybrid analysis technique that utilizes SdH and PL data to accurately determine the 2D gas concentration in PHEMT structures with multiple subband occupation and with severe parallel conduction due to the heavily doped contact layer. The technique requires B sweeps of only a few tesla, is noise tolerant and is much faster than iterative-etch techniques. Results of the new technique are shown to yield excellent agreement with the results of established measurement techniques. Because low-temperature PL and Hall-effect measurements are routinely used to characterize device material, no additional device processing or testing is required to implement the hybrid SdH-PL analysis technique. Furthermore, it is easily implemented for automated computer analysis and should prove useful in both research and industrial environments.

Melissa A. Cavaliere is acknowledged for device fabrication and Ted Castillo is acknowledged for SdH measurements. This work was supported by the Department of Energy under Contract No. DE-AC04-76DP00789.

¹H. Brugger, H. Müssig, C. Wölk, K. Kern, and D. Heitmann, Appl. Phys. Lett. **59**, 2739 (1991).

²C.-S. Chang, H. R. Fetterman, and C. R. Viswanathan, J. Appl. Phys. **66**, 928 (1989).

³M. Santos, T. Sajoto, A. Zrenner, and M. Shayegan, Appl. Phys. Lett. **53**, 2504 (1988).

⁴R. D. Larrabee and W. R. Thurber, IEEE Trans. Electron Devices **ED-27**, 32 (1980).

⁵D. Weiss and K. v. Klitzing, in *High Magnetic Fields in Semiconductor Physics*, edited by G. Landwehr (Springer-Verlag, Berlin, 1986), Vol. 71, p. 57.

⁶For a comprehensive review, see *The Quantum Hall Effect*, edited by R. E. Prange and S. M. Girvin (Springer-Verlag, Berlin, 1987).

⁷H. Fetterman, J. Waldman, and C. M. Wolfe, Solid State Commun. **11**, 375 (1972). Slightly higher masses have been reported by C. T. Liu, S. Y. Lin, D. C. Tsui, H. Lee, and D. Ackley, Appl. Phys. Lett. **53**, 2510 (1988).